Pharmaceutical Validation

In situ spectroscopic cleaning validation

Aaron A. Urbas and Robert A. Lodder (College of Pharmacy and Department of Chemistry, University of Kentucky, Lexington, KY 40536-0082, USA. E-mail:* lodder@uky.edu*)*

The US Food and Drug Administration (FDA) has noted that US drug products are of generally high quality, but there is an increasing trend toward manufacturing-related problems that lead to recalls, disruption of manufacturing operations and loss of availability of essential drugs. Low manufacturing process efficiency has also led to increased cost of drugs. Emphasis on cGMP (current good manufacturing practice) as the means of controlling drug quality has led to reluctance among companies to innovate in the manufacturing sector. Such problems have led the FDA to conclude that a new scientific understanding of the drug production process achieved through the use of new sensing technologies can provide science-based approaches to the regulation of drug quality, thereby alleviating these problems. Process analytical technologies (PAT) like near infrared (NIR) spectroscopy have been selected as the model for the US to use in shifting successfully from empirical standards like cGMP to science-based standards for achieving manufacturing-process quality. One area in which PAT may foster process understanding is cleaning validation.

In the past decade, the issue of validating cleaning procedures in pharmaceutical process equipment has grown significantly. This rise in interest has, in part, been driven by an increased attentiveness to cleaning validation by regulatory bodies.[1–3] The objective of cleaning validation is simple: accurately verify that potentially harmful compounds have been removed (below acceptable limits) from surfaces in process equipment prior to its use for another purpose. In the pharmaceutical industry this arises primarily when equipment is used for processing two or more active pharmaceutical ingredients (APIs), where cross-contamination can have severe consequences. Of further concern in these applications is the removal of the agents used in the cleaning process. The two most prevalent methods for accomplishing these tasks are analysing residues collected by swabbing a predetermined portion of the surface and analysing the rinse matrix collected after a surface has been cleaned.[4–8]

Although these methods have proven successful, there are several shortcomings. Drawbacks with swabbing, the most commonly used technique, include the need to sample the surface, incomplete analyte recovery from surfaces, analyte extraction requirements after swabbing. Additionally, the procedure is time consuming, resulting in lengthy downtimes for processing equipment. Rinse testing can be used as an alternative or complementary method and allows for collection from the entire surface. This method suffers from limitations as well, including more difficult method validation and analyte solubility/surface detachment issues. An additional drawback to these two methods is the fact that the quantity of analyte remaining on the surface must be estimated from the analysis of the samples drawn.

An ideal validation method for cleaning procedures would be a rapid, automated, *in situ*, multi-component analysis of the entire surface. With this approach, errors and inadequacies associated with surface sampling procedures would be eliminated. The use of spectroscopic techniques for *in situ* determination of contamination on surfaces is not new.[9] In general, these previous studies lack the sensitivity or selectivity that is required for a cleaning validation application. However, recent work, using the mid-IR spectral region and fibre optics has provided a spectroscopic instrument capable of *in situ* surface contaminant analysis with cleaning validation being a specific aim.[10] NIR spectroscopy has the potential to be useful in this type of approach to cleaning validation. Several appealing aspects of NIR spectroscopy for this approach are the ability to discriminate components, rapid analysis time and the capability for *in situ* analysis. One disadvantage to the use of NIR for cleaning validation is the need for low detection/quantification limits (in the sub-μg cm^{-2} range). This problem may be alleviated in part with the use of laser sources and hyperspectral imaging. Even with these powerful sources, though, accurate quantification and spatial resolution of the analyte or analytes of interest on surfaces may be difficult with traditional NIR reflectance measurements alone. A hyperspectral UV/visible/NIR approach to this problem may be necessary to achieve acceptable results. Such a method has already been employed to monitor bacterial film growth on surfaces.[11]

We have recently begun work to develop a multifunctional active-excitation spectral analyser capable of illuminating a spot or line on a surface and examining the returned light for multiple spectroscopic phenomena such as absorbance, scattering, polarisation and luminescence. Multiplexing the spectroscopic techniques offers the potential to create an accurate surface-scanning instrument capable of multi-component analysis with wide applicability in cleaning validation and other applications. This idea was partly inspired by a similar device, a multifunctional active excitation spectral analyser (MAESA), developed for materials characterisation on planetary probes.[12] The MAESA operates by illuminating a remote point or line with a laser beam, and is capable of analysing the returned light for traditional visible and NIR spectral information as well as Raman scattering phenomena. The instrument operates at near room temperature and has a wavelength response range from 0.5 to 2.5 μm. The MAESA approach is amenable to automation for scanning of surfaces to provide remote spectrometric analysis for cleaning validation.

Preliminary work in the concept-development stage of this project began with an experiment to predict concentrations of bovine serum albumin (BSA) on microscope slides by examining the scatter from an incident red HeNe laser beam (632.8 nm). The laser beam passed through a sample slide, striking the “dirty” surface of the slide first. To improve sensitivity, the bulk of the laser beam (i.e. the unscattered portion of the light) was allowed to pass through an aperture in the image plane to a beam dump. The spatial filter created by the aperture and beam dump reduced the dynamic range of the light scattering intensity on the image plane that needed to be captured by the camera A/D. Slide samples were prepared by spreading known volumes of dilute aqueous solutions of BSA as evenly as possible into the oval wells of Teflon

printed microscope slides (24.4 by 16.7 mm single oval well, Electron Microscopy Sciences, Fort Washington, PA, USA) to generate a series of 11 slide samples with known surface-BSA concentrations ranging from 0 to 20 µg cm^{-2}. Thirty light scattering images were collected for each slide in a raster fashion to scan as much of the slide surface as possible. The angle of the incident laser beam was optimised in a previous experiment at 15° to the slide's surface to maximise between-sample separation of the light scattering images. (These results will be discussed in a future publication but cannot be discussed here due to space limitations.) An Olympus D-520 Zoom digital camera (Olympus Optical Co. Ltd, Tokyo, Japan) was used to collect the light scattering images and was fixed throughout the experiment at approximately 45° to the image plane of the spatial filter to allow direct comparison of all images. Images were initially collected as 1600 × 1200 pixel JPEGs, but due to computer processing constraints the images were resized to a maximum of 400 × 300 pixels by Adobe Photoshop LE (Adobe Systems Inc., San Jose, CA, USA). The data used for each image were obtained by extracting the red channel from the reconstructed RGB images (see Figure 1). Principal component regression (PCR) was used in this work to generate calibration models to predict BSA concentration from scattering images.

With this setup there are two kinds of images: the "scattering image" collected from a single point on the BSA slide, and the "slide image" reconstructed by the MAESA program from an ensemble of scattering images obtained at different locations on the slide surface. The slide image depicts the location and concentration of BSA on the slide surface. The light scattering images showed that the concentrations of BSA were not uniform across the slide surfaces as the extent of scattering varied widely for a single slide. The ability of the instrument to quantify BSA on slide surfaces was determined by averaging scattering measurements on a slide image. Scattering images were also averaged (smoothed) using groups of pixels in the images. The effect of scattering image resolution was also investigated by looking at image resolutions ranging from one pixel (calculated by the mean of all pixel values of the images) up to 400 × 300 pixels. Briefly, the prediction accuracy was nearly constant down to scattering image resolutions of 25 × 19 pixels, below which there was a marked increase in the BSA prediction error. This result illustrated that for the equipment used in this study, the spatial distribution of the light scattering was important for accurate BSA prediction. The total amount of light scatter (as might be obtained with a single element detector instead of an array) was not enough to achieve a good BSA prediction.

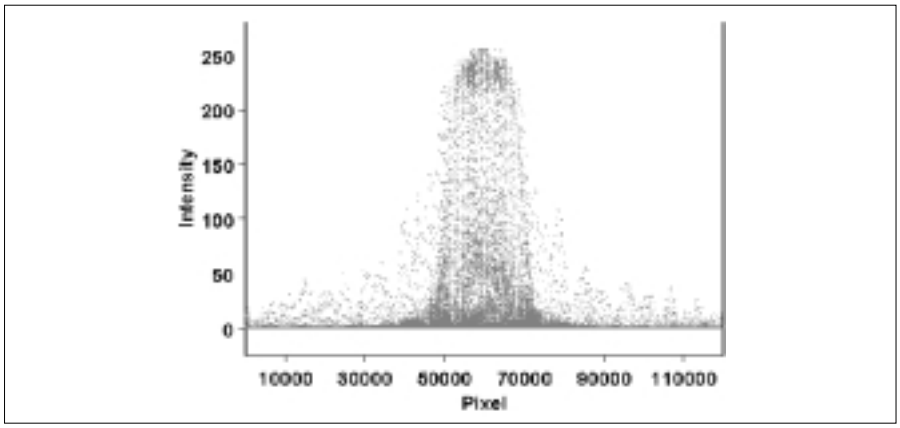

Figure 1. The distribution of signal intensities in a single scattering image. The aperture for the spatial filter was located at 60,000 on the x-axis.

The BSA prediction accuracy was first scrutinised by looking at the average of the scattering images (400 × 300 resolution) for each slide image. The red-channel scattering-image data were treated as a 120,000-dimensional spectrum and a principal component (PC) transformation was performed. It was apparent from the PC scores that there was a non-linear relationship between BSA concentration and scattering intensity and distribution. Therefore, a second-order polynomial fitting routine was used to generate prediction models. These second-order models significantly outperformed the simple first-order models on cross-validation. Figure 2 shows the cross-validation results obtained using a second-order model. For this graph, the r^2 was 0.9990 and the standard error or prediction (*SEP*) was 70 ng cm^{-2} (*SEE* = 50 ng cm^{-2}, 0.35% relative *SEP* over the range of concentrations, cross-validation with the f test at $p = 0.05$).

The effect of the number of scattering images averaged on the prediction precision was also examined. A graph of

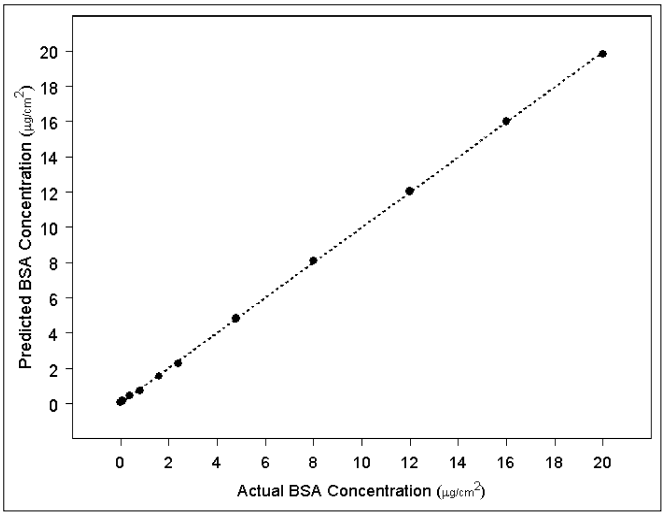

Figure 2. Prediction of BSA concentration using single-wavelength laser light scattering measurements. r^2 = 0.999, *SEE* = 50 ng cm^{-2}, *SEP* = 70 ng cm^{-2}.

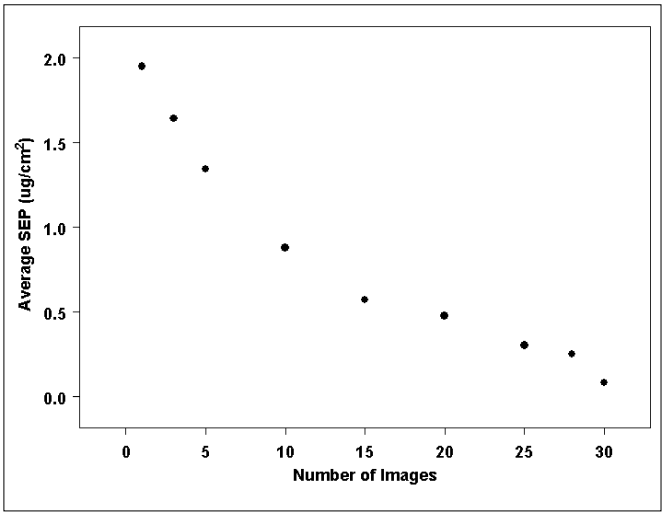

Figure 3. The effect of the number of scattering images averaged to form a slide image on the precision (*SEP*) of BSA prediction.

the leave-one-out cross-validation prediction precision vs the number images averaged is presented in Figure 3. To generate each point on this graph, the specified number of scattering images for each slide were randomly selected and averaged, then calibrated, and a cross-validation routine was used to find the *SEP*. The averages for 10 repetitions of this procedure are shown in the graph, with the exception of the final point (30 images), as there is only one possible data set for this point. This graph was generated with 400 × 300 scattering images, but the analogous data for 25 × 19 images are very similar. Figure 3 shows a general decrease in prediction error as the number of images averaged is increased. As mentioned previously, examination of the individual images leads us to believe that this trend is in large part due to uneven BSA distribution across the slides surface and not due to noise or other experimental variations.

Conventional NIR spectrometry of BSA-contaminated slides was not nearly as sensitive to changes in BSA concentration. Scanning 12 slides covering a concentration range of 0–727 µg cm^{-2} from 1100 to 2500 nm with a conventional monochromator instrument (InfraAlyzer 500, Bran+Luebbe) produced a calibration with an *SEE* = 8 µg cm^{-2} and an *SEP* = 21 µg cm^{-2} (f test at $p = 0.05$). The major peaks in the PC loadings (PCs 1–4) were all between 2000 and 2150 nm. Scanning the same slides used for the laser calibration (0–20 µg cm^{-2}) showed little significant correlation between the spectra and the BSA concentration. While BSA absorbance signals are more intense in the NIR, scattering signals are greatly reduced.

The results of this experiment demonstrated that BSA concentrations on glass surfaces can be accurately assessed by examining light scatter from these surfaces. The major limitation to this work though is that BSA was the only component present on the glass surfaces, a situation that is not very common in cleaning validation applications. Plans for future work on this project are numerous. Multiple component systems will be analysed that include APIs, cleaning agents and excipients using hyperspectral MAESA. Analysis on other surfaces such as stainless steel will be investigated. Finally, investigations with polarisation and luminescence will be performed.

References

1. ICH, *Q7A Good Manufacturing Practice Guidance for Active Pharmaceutical Ingredients*. International Conference on Harmonisation of Technical Requirements for Registration of Pharmaceuticals for Human Use (2001).
2. PhRMA Quality Committee, BPWG, *Pharm. Technol.* **21(9),** 56 (1997).
3. FDA, *Guide to Inspections of Validation of Cleaning Processes*. Food and Drug Administration: Washington, DC, USA (1993).
4. L. Westman and G. Karlsson, *J. Pharm. Sci. Technol.* **54(5),** 365 (2000).
5. D.A. LeBlanc, *Validated Cleaning Technologies for Pharmaceutical Manufacturing.* Interpharm Press, Englewood, CO, USA (2000).
6. G. Bismuth and S. Neumann, *Cleaning Validation: A Practical Approach*. Interpharm Press, Englewood, CO, USA (1999).
7. D.A. LeBlanc, *Pharm. Technol.* **22(5),** 66 (1998).
8. K.M. Jenkins and A.J. Vanderweilen, *Pharm. Technol.* **18(4),** 60 (1994).
9. P. Lilienfeld, *Aerosol Sci. Technol.* **5(2),** 145 (1986).
10. N.K. Mehta *et al.*, *BioPharm* **15(5),** 36 (2002).
11. Amanda E. Lowell, Kah-Siew Ho and Robert A. Lodder, *Remote Hyperspectral Imaging of Endolithic Biofilms Using a Robotic Probe, Contact in Context:v1i1/planetprobe*, http://cic.setileague.org/cic/v1i1/planetprobe.pdf, pp. 1–10.
12. K. Quiesup, *NASA TECH BRIEF* **26(1),** i, 1-2, 1a-18a (2002).